The Bainite Transformation in a Silicon Steel
H. K. D. H. Bhadeshia and D. V. Edmonds
Metallurgical Transactions A, Vol. 10A, 1979, pp. 895-907.

(I.1) Introduction

The bainite transformation remains the least understood of all the decomposition reactions of the high temperature austenitic phase in steels. The complexities of its formation mechanism and kinetics, and the apparent diversity in its microstructural appearance, even create disagreement in identifying its correct definition (1,2). However, the well known difference in carbide distribution between bainite formed at high and low temperatures, viz., intralath and interlath, respectively, appears to exist in a majority of steels and makes the classical nomenclature of upper and lower bainite useful, both in describing the microstructural appearance and in classifying the overall reaction mechanism (3-9). In this respect, these terms are used in the present work.

Since bainite forms in the temperature range dividing the reconstructive ferrite/pearlite reactions and the displacive martensitic reaction, there has been a natural desire to relate bainite to one or other of these phases, which has led to much controversial debate concerning the mechanism of its formation (1,10-14).

One school of thought considers that the ferritic component of bainite develops over the whole bainitic temperature range by a diffusional ledge mechanism analogous to the proposals made to account for the formation of widmanstätten proeutectoid ferrite (1). The carbon content of this ferrite is considered to be between the $\alpha/\alpha+\theta$ and the extrapolated $\alpha/\alpha+\gamma$ phase boundaries, and bainitic carbides are considered to form primarily at the austenite/ferrite interface (1). Recent detailed electron diffraction studies of the carbide precipitation reactions have been interpreted to give support to this hypothesis (13). A solute drag model is invoked to explain the bay in the TTT curve at the B_s temperature (15). The incomplete reaction characteristic of the bainite transformation (1,16) is claimed not to be a general phenomenon (1).

The opposing school of thought considers the bainite reaction to be a displacive transformation (involving an atomic correspondence) controlled essentially by the rate at which composition change is accomplished by carbon removal to the surrounding austenite, or by some other rate controlling process such as

strain energy relaxation (1,10,11,16). It is expected that the austenite/ferrite interface should exhibit the same characteristics as in the martensitic transformations. The ferritic component of bainite is thus thought to form with a carbon supersaturation (10,16,17) which in lower bainite is essentially relieved by carbide precipitation within the ferrite. This reaction is thus analogous to autotempered martensite. The existence of a metastable eutectoid reaction controlling the carbide precipitation event has also been postulated (16). This concept is also extended to support the idea of a discontinuous change from upper to lower bainite at a temperature of 350°C virtually independent of the steel composition. The B_s temperature is considered to be due to the intersection of two separate C-curves for reactions (i.e. widmanstätten ferrite and upper bainite) occurring by fundamentally different mechanisms(1,18).

The present chapter describes a study of the bainite reaction in a steel containing deliberate additions of Mn and Si. The importance of the silicon addition in this respect is that it inhibits the formation of cementite, which is the critical event in the progress of the bainite reaction since it removes carbon from the austenite or ferrite. Thus, despite being classified as a ferrite forming element, the presence of Si during the bainite reaction leads to incomplete transformation. The further addition of Mn to the alloy helps to stabilise the untransformed austenite at room-temperature, and also to impart sufficient hardenability for heat treatment. The presence of retained austenite and the slower progress of the overall bainite reaction allows a more thorough study of the transformation mechanism.

(I.2) Experimental Procedures

A 65g melt of the experimental alloy was prepared from pure constituents in an argon-arc furnace, and the final chemical analysis was Fe-0.43C-3.00Mn-2.12Si wt. pct. The ingot was sealed in a quartz capsule under a partial pressure of argon and homogenised for three days at 1250°C, before hot-swaging to 3mm diameter rod.

Austenitising treatments (generally 5mins. at 1200°C) were carried out with the specimen sealed in a quartz capsule. Subsequent isothermal heat treatments were carried out by fracturing the quartz and quenching into a tin bath covered with a layer of active charcoal.

Thin foil specimens for transmission electron microscopy were

prepared from 0.25mm thick discs slit from the heat-treated 3mm diameter rod under conditions of flood lubrication. The discs were subsequently thinned and electropolished in a twin-jet polishing unit using a 5% perchloric acid, 25% glycerol and 70% ethanol mixture at room temperature and 55 volts. The foils were examined in a Philips EM300 transmission electron microscope operated at 100kV.

Dilatometric analysis was carried out on a Theta Industries high-speed vacuum dilatometer using a 20mm by 3mm diameter tube specimen with a 1.5mm diameter bore to facilitate fast cooling. Quenching to the isothermal transformation temperature was achieved by an automatically controlled high-pressure helium jet directed both radially and axially at the specimen. No significant decarburisation occurred.

X-ray analysis was carried out on 1.5mm thick flat-rolled specimens which had been chemically thinned to remove approximately 0.3mm of material from the surface subsequent to heat treatment. A Philips horizontal diffractometer with Co radiation and a LiF crystal monochromator in the diffracted beam was used.

(I.3) Results and Discussion

(i) Reaction Kinetics

Dilatometry combined with optical and electron microscopy was used to determine the bainite TTT curve. Figure I.1 shows the 5% transformation curve; the dashed lines indicate the scatter obtained and it is thought that this scatter is real since it exceeds the estimated experimental errors. Since transformation was usually incomplete, calibration for the total length change due to 100% transformation was obtained by first transforming to upper bainite at 350°C followed by a temper at 500°C in order to decompose the retained austenite. The two length changes measured were then added, after allowing for thermal expansion, in order to obtain the length change due to 100% transformation. Separate C-curves were indicated for upper and lower bainite*, and this is

* Throughout this study upper bainite is defined as an aggregate of bainitic ferrite and high-carbon retained austenite without any carbide precipitation due to the influence of the high level of silicon in the experimental alloy. Lower bainite is defined as an aggregate of bainitic ferrite with little retained austenite and, distinctively, intralath precipitation of sheet-like cementite particles in the ferrite. Justification for these definitions will become evident in the section on microstructural observations.

considered further below.

Electron microscopy revealed that the upper and lower bainite reactions did not go to completion despite prolonged periods of holding at the isothermal transformation temperature (significant amounts of retained austenite were detectable in all cases).

It was found that near the B_s temperature only a very limited amount of austenite transformed to bainite despite holding at the isothermal transformation temperature for 32 hours. Dilatometry indicated an initial limited amount of rapid transformation followed by an asymptotic termination. Figure I.2 shows a specimen isothermally transformed at 452°C for 32 hours and it is clear that only a small amount of upper bainite has formed and that eventually the pearlite reaction has taken over.

The temperature dependence of the 'incomplete reaction' was investigated by measuring the length change from zero time to a time when the reaction rate was negligible ($dL/dt = 7.6 \times 10^{-6}$ cm s^{-1}). This data is plotted as a function of the isothermal transformation temperature in fig.I.3. It is clear that the extent of transformation is a sensitive function of the incomplete reaction phenomenon (16). This data is considered to be particularly relevant since there is no interference from carbide precipitation during the upper bainitic ferrite reaction in this alloy. Any precipitation of carbide would naturally reduce the carbon content of the enriched austenite, thereby promoting further transformation.

The extra bays indicated by high-speed dilatometry in the bainite TTT diagram between the upper and lower bainite reactions, and between the lower bainite and martensite reactions have not been detected before and required further confirmatory studies. Quenching into a tin bath held at the required isothermal transformation temperature failed to reveal metallographically the lower part of the upper bainitic curve due to the onset of the lower bainite reaction. However, it was found that when helium quenching was used (in the dilatometer) the lower part of the upper bainitic curve was well defined (e.g. figure I.1), and metallography specified a temperature region where either upper bainite or lower bainite formed but never a mixture of the two. This indicated a dependence of the transformation product (upper or lower bainite) on the quench rate to the isothermal transformation temperature. It appeared that upper bainite would form when the quench rate was relatively slow. Step

quenching experiments were conducted to verify this. Following austenitisation, specimens were quenched to the metastable bay (500°C) above the B_s temperature and held for 30 seconds before quenching into a tin bath at a temperature in the lower range of the upper bainitic C-curve (283°C). This treatment effectively reduces the quench rate to the isothermal transformation temperature. Very little transformation to a typically feathery upper bainite product was recorded, and electron microscopy confirmed upper bainite consisting of bainitic ferrite and retained austenite in a bulk matrix of martensite (figure I.4). The existence of a separate C-curve for the upper bainite reaction was therefore confirmed in detail and a quench rate effect was noted such that upper bainite was obtained at low quench rates (to isothermal transformation temperature) in the region of overlap of the upper and lower bainite reactions.

Isothermal transformation at 247°C revealed the lower part of the lower bainitic curve; very little transformation was detectable metallographically despite relatively long periods at the isothermal transformation temperature (figure I.5). It is noted that the dilatometrically determined M_s temperature of this alloy is 220°C. It was found that a significant slowing down of reaction kinetics corresponding to the upper part of the lower bainitic C-curve could not be detected with confidence.

By the kinetic definition the bainite reaction has its own C-curve; as the maximum temperature of this curve (the so-called kinetic B_s temperature) is approached, the proportion of bainite formable decreases (ideally) to zero (1). In alloy steels there is usually a well defined bay at the B_s temperature above which austenite will not transform by the bainitic mode. The present results are consistent with this definition and, because of the agreement between the dilatometry and optical and electron microscopy, also indicate that the kinetic definition is directly equivalent to the microstructural B_s. The existence of separate reaction curves for the upper and lower bainitic transformations is also observed.

Based on kinetic observations of an Fe-Mo-C alloy, Aaronson concludes that the kinetic-B_s is only a manifestation of the special effect of alloying elements on the growth kinetics of proeutectoid ferrite (1,2) i.e. the minimum in growth kinetics is interpreted in terms of a drag effect produced by the segregation of certain alloying elements to the austenite/ferrite

interfaces. It is suggested that alloying elements which decrease the activity of carbon in austenite should exercise an enhanced drag effect relative to those that do not (2,15) and the absence of a bay in an Fe-C-1.0Mn a/o alloy is claimed to be consistent with the relatively small effect of Mn in reducing the carbon activity in austenite (15). It is further claimed that elements such as Si and Co which raise the activity of C in austenite should not give rise to the kinetic-B_s phenomenon (2). In plain carbon steels the kinetic features are not well defined although several other features of the bainite reactions are present. Depending on the theory subscribed to, diffusional ledges or displacive shear, this can be attributed either to observational difficulties (related to competition from the pearlite and proeutectoid ferrite reactions) (1) or to the absence of any substitutional solute elements to exert a drag on the transformation front (1).

According to Aaronson (2) the development of the bainite reaction below the B_s temperature can be visualised in terms of the competition between the reaction driving force and the approach to saturation of the solute drag effect.

The present results would appear to be inconsistent with the solute drag model which can only explain a single bay in the vicinity of the B_s temperature, and not the three observed in the present work. Recent work (19,20) has added the possibility that the so-called "solute drag effect" may simply be due to the influence of carbide precipitation on the dynamics of the austenite/ferrite interface in the region of the kinetic bay.

Based on available thermodynamic data (21) it is concluded that the composition of the present alloy merits a large increase in the activity of carbon in austenite. Despite this fact, a strong kinetic B_s is observed, in contradiction to the above solute drag model; furthermore, electron microscopy clearly shows the absence of any carbide precipitation at this temperature.

The alternative explanation is that the B_s temperature arises from a fundamentally different mechanism of the bainite reaction as compared to the formation of widmanstätten ferrite (1,10,14,16). Additionally, supporters of the theory that bainite forms by a displacive shear mechanism also postulate that it 'forms' by the repeated nucleation of substructural units that propagate rapidly to a limited size, and thus the incomplete nature of the

reaction can be attributed to a restriction on nucleation rather than on growth. Consistent with this observation is that upper bainite plates retain their lenticularity; they do not appear to thicken following their initial rapid formation. There is, however, only limited evidence for the existence of these substructural units, especially for the case of upper bainite (10) and the explanation of the incomplete reaction phenomenon in terms of a link between the relaxation of accommodation strains and the nucleation event is tenuous and unconvincing. Speich (22) points out that the major component of the accommodation strains would not be relieved by the partitioning of carbon - the latter would only lead to a volume contraction and not reduce the important shear component of the total shape strain. In the present work, evidence for the sub-units referred to above is presented for upper and lower bainite in the section on microstructural observations and an explanation of the incomplete reaction phenomenon is dealt with in detail in chapter two.

The two separate C-curves for upper and lower bainite observed in the present study are also thought to arise from two distinct transformations operating in each case and the lower parts of the two C-curves may then be attributed to the increasing difficulty of dissipating the carbon diffusion fields of the prior sub-units (this will become clear in the context of chapter two).

(ii) Microstructural Observations - Upper Bainite

Isothermal transformation in the upper bainitic temperature range (defined by dilatometry) always gave an aggregate of bainitic ferrite and retained austenite (figure I.6). There was no detectable carbide precipitation even after holding at 350°C for 74 hours. As indicated by previous investigators (23-25), this clearly results from the presence of Si. Si is known to inhibit cementite formation during the tempering reaction in steels (23-25). This is generally explained by the relative insolubility of Si in cementite requiring the diffusion controlled ejection of Si at the transformation front which in turn results in a Si concentration build-up during an early stage of growth. This locally increases the activity of carbon so that the carbon flux is reduced and further development of the cementite embryo is inhibited (23). However, it should be noted that even high resolution electron microscopy failed to reveal any carbide in the upper bainite involved in the present study.

Prevention of cementite formation correspondingly leads to a high concentration of carbon in austenite. Stabilisation of the austenite at room temperature indicates that at some stage during the bainite reaction the austenite becomes enriched with respect to carbon. Whether the bainitic ferrite forms with a supersaturation in carbon, and if so, at which stage of the reaction the partitioning of carbon to the austenite takes place, is a matter of keen dispute (e.g. ref.1). Furthermore, although carbon must play a vital role in the stability of this austenite, it is likely that other physical factors also contribute to this and to the overall extent of transformation; this point is dealt with further in the discussion of the X-ray diffraction experiments. For the purpose of a detailed metallographic study it was found that 30 minutes at 350°C allowed sufficient reaction, and hence adequate carbon enrichment to stabilise the austenite for subsequent room temperature examination. This does not imply that zero austenite is retained when the extent of transformation is low because regions of austenite which become totally surrounded by bainitic ferrite achieve the required carbon content (e.g. figure I.4).

The interwoven or branching nature of the bainitic ferrite/retained austenite aggregate is shown in figures I.4,6 and is characteristic of the upper bainite morphology in similar steels containing Si additions (13). It is interesting to speculate how bainitic 'plates' could have formed with internal films of austenite to give an irregular composite character to each individual macroscopic plate. Although interrupted by the austenite regions, the ferritic components of the plate are semi-continuous and in the same crystallographic orientation. It is clearly difficult to see how the plates could have thickened to this morphology by the progression of ledges along the planar interfaces parallel to the long direction of the plates. Rather, the regular partitioning of the plate along its length by the austenite fingers emanating from the main austenite lamellae is more suggestive evidence for the formation of bainitic ferrite by 'martensitic jumps' composed of smaller units. This aspect will be developed further in chapter two.

During the course of electron metallography it was observed qualitatively that the bainitic ferrite contained a high dislocation density, and that this was higher than that of the retained austenite. Clusters of dislocations could also be found associated with the austenite/ferrite interfaces (figure I.7a).

The Bainite Transformation in a Silicon Steel
H. K. D. H. Bhadeshia and D. V. Edmonds
Metallurgical Transactions A, Vol. 10A, 1979, pp. 895-907.

The retained austenite was also found to contain planar faults, very often with one dominant fault plane (figure I.7b). When the fault plane was approximately normal to the foil plane, the faults could be seen to terminate at slip steps in the austenite/ferrite interface (figure I.7c). It is attractive to suggest that these steps are indicative of accommodation slip on $\{111\}_\gamma$ planes in the austenite phase during a displacive transformation.

A series of specimens was given different austenitising treatments before transforming to upper bainite for 115 minutes at 350°C. Varying both the austenitising temperature and time gave a range of austenite grain sizes and also corresponding changes in austenite texture (due to selective grain growth). The isothermal treatment chosen allowed the bainite reaction to proceed to an extent sufficient to stabilise untransformed austenite at room temperature. The austenite levels were sufficient for accurate X-ray analysis (Table I.1).

The volume fraction of retained austenite was calculated from the X-ray intensities; texture effects were taken into account in accordance with the work of Dickson (26) by utilising the integrated intensities of a minimum of three ferrite and three austenite peaks. Experimentally determined lattice parameters were used in each case since these were expected to vary with the degree of transformation due to the partitioning of carbon into the austenite; different structure factors thus had to be calculated for each specimen. The accuracy of the lattice parameter calculations was maximized by the use of an extrapolation function (27).

The results of the analysis may be interpreted as follows: $P_{hkl} = 0$ corresponds to a random orientation, $P_{hkl} < 1$ shows that such $\{hkl\}$ planes are preferentially avoided and $P_{hkl} > 1$ means that these planes are preferentially oriented parallel to the plane of section** .

** $P_{hkl} = (I_{hkl}/R_{hkl})/\frac{1}{n}\sum^{n}(I/R)$

where I = integrated intensity of the reflection concerned,
and R = correction factor for each reflection as defined in ref.26.

The prior austenite grain diameter (d) was also measured by lineal analysis on the actual specimens used for the X-ray determinations. The correlation between the volume fraction of retained austenite and grain size proved to be rather poor

with the best correlation coefficient of 0.56 obtained against d^{-3}.

In view of this rather poor correlation the data was examined in greater detail and it was thought that texture was affecting the degree of transformation. To test this hypothesis, the pct. retained austenite was examined as a function of P_{111_γ} and d^{-3}. It was found that a drastically improved multiple correlation coefficient was obtained when the pct. retained austenite was plotted as a function of both the above variables. However, the multiple correlation coefficient was further increased to 0.981 when P_{110_α} was used instead of P_{111_γ}, (figure I.8). This is probably so because the textured austenite $\{111\}_\gamma$ planes are not necessarily faithfully replicated by the ferrite $\{110\}_\alpha$ planes during transformation.

In view of the excellent correlation, it is concluded that the texture of the $\{111\}_\gamma$ planes has a significant effect on the extent of transformation. Since the $\{111\}_\gamma$ planes are the most common slip planes in austenite, this effect is consistent with slip in the austenite during transformation; that its importance is revealed through a texture effect is probably because of a greater possibility of cooperative transformation between adjacent grains with an increase in the $\{111\}_\gamma$ texture. Certainly, in the initial nucleation event, irrespective of the final details of the transformation crystallography, the close-packed planes are considered to be of fundamental importance in generating the BCC lattice from the FCC lattice (28). One would thus expect a decrease in the amount of retained austenite with an increase in the degree of cooperative formation, as manifested by the P_{111_γ} and P_{110_α} values.

The strong correlation of P_{111_γ} with pct. retained austenite rather than any of the other low index austenite planes emphasises the importance of $\{111\}_\gamma$ planes in the upper bainite transformation. This is consistent with the previous observation of slip steps on $\{111\}_\gamma$ planes in the upper bainitic retained austenite.

The fact that such large variations in the extent of transformation can be attributed solely to physical effects stresses the need to refine thermodynamic theories of phase transformations which often ignore these variables.

Bainitic carbide precipitation is an integral part of the

overall bainite reaction, and in order to study this in the upper bainite reaction in the Si-steel it was necessary to induce decomposition of the retained austenite by tempering at a higher temperature. Tempering at 500°C for less than 30 minutes gave a microstructure consisting of bands of fine carbides separated by 'clean' ferrite (i.e. with a minimum of carbide precipitation), indicating that the carbides had mainly precipitated in the prior austenite regions (figure I.9a). The carbides had a thin plate-like morphology, and due to their extremely small size and close spacing, identification by conventional selected area electron diffraction proved impossible. However, using convergent beam electron microscopy several solvable diffraction patterns were obtained, an example of which is illustrated in figure I.9b. All the diffraction patterns could be consistently indexed to the following monoclinic structure:

$a = 8.096$ Å, $b = 10.41$ Å, $c = 7.00$ Å, $\beta = 107.2°$

It is thought that this phase is probably an iron-silicon-manganese carbide. The identification of this carbide is considered more fully in appendix one.

Further tempering at 500°C led to complete decomposition of the retained austenite (figure I.9c) and replacement of the above monoclinic carbide by cementite (figure I.9d) with the microstructure now appearing somewhat similar to conventional upper bainite. The cementite was concentrated at lath/sub-boundaries, and gave unusual orientation relationships (i.e. inconsistent with any known rational ferrite-cementite orientation relationships). It is thus probable that the cementite precipitated at the monoclinic-carbide/ferrite interfaces, in which case it would be energetically favourable for it to adopt an orientation giving low energy interfaces with both the monoclinic carbide and the ferrite. Since negligible intragranular precipitation occurred in the bainitic ferrite, it was concluded that the carbon content of the ferrite was of the order of 0.03 wt. pct. However, this only shows that the final upper bainitic ferrite is not supersaturated with respect to carbon and gives no indication as to whether it was supersaturated at some earlier stage in the reaction with carbon which subsequently partitioned into the surrounding austenite.

In order to examine the precipitation sites, hot stage electron microscopy was conducted on specimens which had first been transformed to upper bainite (i.e. a lamellar aggregate of

retained austenite and bainitic ferrite). This revealed (figure I.9e) that while some precipitation occurred totally within the austenite, the majority of carbides formed at the austenite/ferrite interface and grew into the austenite. Following this, the boundary pulled away from the line of carbides and this sequence continued repeatedly until the austenite had fully decomposed. In general, due to the thinness of the austenite lamellae, only one or two lines of carbide were observed before austenite decomposition was completed. These results indicate that the majority of upper bainitic carbides nucleate at the austenite/ferrite interface and grow into the austenite, resulting in its diffusional decomposition. It is thought that this sequence is representative of the full reaction to a bainitic ferrite/carbide aggregate in low-Si steels, but that in the latter case the decomposition events must occur virtually simultaneously. In the latter case the transition carbide would probably be epsilon carbide rather than the monoclinic carbide found in the present work. This would be consistent with the Isaichev orientation relationship generally observed between the cementite and bainitic ferrite in low-Si steels (29) since the crystallography of epsilon carbide/ferrite is closely related to that of cementite/ferrite when the latter corresponds to either the Isaichev or the Bagaryatski orientations (30). Hence, in steels where intermediate carbides are stabilised relative to cementite, there is a clear possibility that the final upper bainitic cementite is really the result of a sequence of carbide precipitation events. In other steels such a sequence would perhaps be too rapid to detect, if it existed at all.

(iii) **Microstructural Observations - Lower Bainite**

Isothermal transformation in the lower bainitic temperature range also resulted in an aggregate of ferrite and retained austenite, although the amount of retained austenite was very much lower than obtained in the upper bainite reaction. The lower bainite microstructure was, however, distinctly characterised by the presence of carbide precipitation within the bainitic ferrite plates (figure I.10a).

In contrast to upper bainite, the individual ferrite plates in the lower bainite are more regular. The dislocation content of the ferrite was higher than in the retained austenite, and also higher relative to upper bainitic ferrite. Furthermore, regular dislocation arrays were occasionally observed, with dislocation lines appearing parallel to the traces of the sheets of carbide

precipitates, implying, as will be seen later, that the dislocations could lie on $\{110\}_\alpha$ planes (figure I.10b).

The ferrite plates very occasionally showed twinning (figure I.10c) on a single variant of the twin plane which appears very similar to the twins observed in the martensite in this alloy. Studies of martensite in this alloy have shown that these martensitic twins are on $\{112\}_{\alpha'}$ planes (Ch.7). When the austenite-martensite matrix-martensite twin lattices are superimposed in the correct relative orientations, the $\{112\}_{\alpha'}$ planes correspond to different planes in the austenite lattice in different sets of data (the same variant of the correspondence is used in each case) which suggests mechanical twinning rather than transformation twinning (Ch.7). If they had been transformation twins they would all have corresponded to the same austenite plane. While a similar analysis has not yet been conducted for the lower bainitic twins, the morphology, probability of occurrence, and distribution are the same and it is tentatively concluded that they are also mechanical twins. This is considered to be an appropriate conclusion for a supersaturated lower bainitic ferrite; the carbon would be expected to raise the general flow stress relative to the twinning stress, thereby making twinning deformation more likely.

No apparent regularity in the dislocation structure of the retained austenite was detected. Furthermore, the lower bainitic retained austenite did not in general exhibit regular stacking fault arrays (figure I.10d), and the stacking fault density also appeared to be significantly lower relative to the upper bainitic retained austenite. These qualitative observations on the differences in the defect structures of upper and lower bainite provide further evidence for mechanistic differences between the two structures.

Despite the high level of silicon in the experimental alloy, the intragranular bainitic carbide was identified by transmission electron microscopy and electron diffraction to be cementite, even at the very earliest of transformation times (2 minutes at 300°C), and at the lowest of transformation temperatures (247°C). The cementite displayed a distinctive sheet like morphology (figure I.10e), similar to that often obtained in tempered martensites. It is noted that in this alloy there can be no confusion between auto-tempered martensite and lower bainite since electron microscopy revealed that the martensite did not contain

carbides, and negligibly small quantities of retained austenite were associated with the martensite obtained by direct quenching (figure I.11). (Additionally, the martensite in the present alloy tempers initially to epsilon carbide and subsequently to cementite (Ch.4) but the results that follow demonstrate that the starting precipitate in lower bainite is cementite.)

Epsilon carbide was not detected at any stage of the lower bainite reaction. This may be attributable to the high level of manganese in the experimental alloy, which would tend to stabilise cementite; manganese is very soluble in the cementite lattice and also forms Mn_3C which has a structure isomorphous with cementite (31). This result is also consistent with the dilatometric data which showed no contraction associated with the tempering of lower bainite; a contraction is expected if epsilon is present and is eventually replaced by cementite (16).

The absence of epsilon carbide is inconsistent with the interesting concept of a metastable $\gamma \rightleftharpoons \alpha + \varepsilon$ eutectoid reaction (16) proposed to explain the relative temperature insensitivity of the transition from upper to lower bainite to the carbon content of the steel. However, in view of the low diffusivity of Si in the lower bainite temperature range, the cementite must be supersaturated with Si and this leads to the possibility of another metastable equilibrium reaction, i.e. $\gamma \rightleftharpoons \alpha + \theta_{metastable}$. To examine this proposal step quenching experiments were carried out in accordance with the methods of (16). Specimens were partially isothermally transformed to lower bainite and were immediately up-quenched into the γ phase field (time periods up to 15 minutes and temperatures between 350°C and 500°C -i.e. above the alleged eutectoid temperature of 350°C), finally followed by a quench to room temperature. The existence of a metastable eutectoid reaction would require the dissolution of the carbide formed by cooling through the invariant temperature when the system is reheated rapidly to a phase field above that temperature (16). Subsequent examination by thin foil electron microscopy showed that the cementite did not redissolve, and consequently the possibility of a metastable eutectoid reaction based on cementite was also ruled out. Only small volume fractions of lower bainite were involved in the above experiments (0.05-0.10) in order to ensure that the lower bainite was readily in contact with residual austenite and hence allow the carbon resulting from the dissolution of metastable cementite to be easily dissipated into the

residual austenite.

The above results are also supported by the fact that the cementite/lower bainitic ferrite orientation relationship (to be discussed later) found in the present study is different from that observed generally when epsilon carbide is an intermediate phase relative to cementite (31). It can therefore be concluded that the metastable eutectoid, if it exists at all, cannot be a general phenomenon and therefore cannot alone account for the differences between the upper and lower bainite reactions.

Trace analysis showed the cementite precipitate habit plane to be in the vicinity of $\{011\}_\alpha$ in the majority of micrographs analysed although in two specific cases the results were unclear. Up to four different variants of the cementite habit plane have been observed in a single ferrite crystal (e.g. figure I.12a). Analysis of several electron diffraction patterns (an example is given in figure I.12b) revealed an uncommon orientation relationship between the cementite and ferrite matrix , viz.,

$$(011)_\theta \;//\; \{011\}_\alpha \qquad [122]_\theta \;//\; \langle 100\rangle_\alpha$$

However, it was not possible to obtain a rational three phase ($\gamma \succ \alpha \succ \theta \succ \gamma$) crystallography, given the experimentally observed Kurdjumov-Sachs orientation relationship between the austenite and bainitic ferrite. (It should be noted that when carbides precipitate at the interphase interface, a rational three phase crystallography is generally observed -ref. 32).

It was also observed that isothermal transformation for short periods showed a generally low precipitate density, and that often some of the lower bainitic ferrite did not contain detectable carbide precipitates at all (e.g. figure I.12c). This observation along with the multi-variant habit plane and orientation relationship is strong evidence for the hypothesis that the cementite precipitates from a supersaturated matrix. Thus, the often suggested possibility (1,33) that the lower bainitic carbides form at the austenite/ferrite interface is discounted.

The corollary to this argument is that the lower bainitic ferrite does form with a carbon supersaturation which is subsequently relieved by carbide precipitation. However, it may or may not form with a full supersaturation since enriched retained austenite is still obtained. This point will be dealt with in chapter two. From carbide volume fraction measurements the supersaturation is <u>estimated</u> to be 0.25-0.3 wt. pct. C.

It is clear that at the reaction temperatures involved the lower bainitic cementite formation could not possibly have involved any diffusion of iron atoms or of substitutional atoms. It is therefore believed that the cementite must initially form with a supersaturation of silicon so that the growth barrier posed by the build up of silicon at the cementite/ferrite interface does not arise. A detailed examination of the positions of iron atoms in the ferrite lattice and the cementite lattice (figure I.12d) for the observed orientation relation shows that only small atom shuffles are required to generate the cementite lattice from the ferrite lattice. Furthermore, the stacking sequence of the $\{110\}_\alpha$ planes is the same as for the $\{022\}_\theta$ planes after allowing for the shuffles. This is entirely consistent with the idea that cementite has formed with a supersaturation of silicon and with a sheet like morphology.

At low magnifications the cementite often appeared wavy. However, high resolution electron microscopy revealed that the individual cementite particles actually consisted of combinations of sheets on different variants of the habit plane (figure I.10e). These components of the individual particles are also in different crystallographic orientation, i.e. the whole particle is not illuminated in dark field imaging, but only those components that lie on the same habit plane. This is the reason why despite the absence of any coincident reflections between different cementite variants, one is able to image parts of precipitates on apparently different habits (figure I.12a). Considering the mechanism of cementite formation, the change in habit plane in individual precipitates could be due to effects of growth accommodation or minimization of carbon diffusion distances. The apparently wavy nature of the carbide phase has in the past been attributed to the consequence of ledge motion (13).

Some interesting observations were made on specimens partially transformed to give lower bainite in a matrix of martensite. Optical microscopy revealed two basic morphologies of bainitic ferrite, one associated with the grain boundaries and the other precipitated intragranularly (figure I.13a). It was found that the edges of the grain boundary phase corresponded to the habit plane traces of the intra-granularly nucleated phase (figure I.13b). Furthermore, the intragranular plates often formed from the grain boundary lower bainite in a morphology not far removed from that of widmanstätten sideplates associated with proeutectoid ferrite allotriomorphs.

The tips of the intragranular plates could be resolved by electron microscopy into a set of spikes (figure I.13c) of approximately 0.2 microns width. No superledges were observed on the planar edges of these plates. Often individual isolated spikes of approximately 0.2 microns width were also observed (figure I.13d); these exhibited all the carbide precipitation characteristics of the plates (i.e. more than one variant of cementite) although some spikes had none or only sporadic cementite precipitates due to the short transformation times involved. These spikes had the same habit plane trace as those at the tips of larger plates.

Spikes could also be associated with the grain boundary nucleated lower bainite (GBLB), as shown in figure I.13e, and again the width of these was ca. 0.2 microns. The traces of these spikes corresponded to the intragranular lower bainite traces (figure I.13b) so that the mechanism of their formation is not considered to be different in the two structures. In some cases all of the spikes terminated at the same position, giving a jagged, step-like appearance to the transformation front, with the width of these perturbations corresponding to ca. 0.2 microns, consistent with that of the isolated spikes (figure I.13f). It is noted that these cannot be mistaken for superledges since they are not on the habit plane but across the plate; the superledge mechanism requires a major component of the ledge motion to lie on the habit plane in order to generate the plate morphology (34).

It is suggested that the observation of spikes at the advancing transformation interfaces of lower bainitic plates provides strong metallographic evidence for the propagation of the lower bainitic reaction by the successive transformation of units of austenite by displacive shear. This proposal is also consistent with the constant width recorded for the shear units, whether on intragranular or grain boundary nucleated plates.

It is considered that the morphological differences in lower bainite arise because of the effect of the austenite grain boundaries in stimulating nucleation so that a larger number of shear units are nucleated adjacent to each other, giving rise to the GBLB structure.

(I.4) General Summary

The Si-containing steel examined in the present investigation was found to exhibit the upper and lower bainite microstructures,

essentially as described classically, although in the case of upper bainite carbide precipitation was prevented by silicon addition. Detailed dilatometry and electron metallography of this bainite provides further experimental evidence which is thought to be pertinent to the differentiation of the two most favoured models proposed for the reaction mechanism. Both the kinetic and structural results obtained appear inconsistent with a growth model based on a diffusional ledge mechanism (as applied more successfully to widmanstätten ferrite).

Separate bainite C-curves have been identified dilatometrically, with a B_s-temperature and incomplete reaction, which with microstructural observations indicated the overlap of separate C-curves for ferrite/pearlite and upper bainite, consistent with transformation by fundamentally different mechanisms. The existence of separate C-curves for upper and lower bainite gives rise to two further incubation bays in the transformation curve which are impossible to explain by special alloying element effects giving interfacial solute drag. Furthermore, the morphology of the upper bainite is difficult to reconcile with its formation by the migration of transformation ledges along the planar partially-coherent faces of the bainitic ferrite plates and is consistent with a displacive mechanism involving the propagation of the transformation by the successive nucleation of displacive sub-units.

The observation of lower bainitic ferrite growth by the apparent formation and coalescence of adjacently nucleated transformation spikes is also consistent with the hypothesis of growth by the repeated nucleation of shear units. Furthermore, the importance of the $\{111\}_\gamma$ slip planes, and the observed defect structures in the retained austenite suggest transformation slip in the parent austenite in upper bainite, whilst the high dislocation density (with some linear arrays parallel to $\{110\}_\alpha$ traces) and occurrence of mechanical twinning in the ferrite suggest accommodation in the product ferrite in lower bainite. These observations not only support formation of bainitic ferrite by a shear mechanism, but are also consistent with the existence of two separate C-curves for upper and lower bainite, and indicative of two fundamentally different mechanisms separated by a very narrow temperature range at approximately 350°C.

The retention of relatively large quantities of austenite and its stability (even in thin foils) suggest carbon enrichment of the parent austenite in both the upper and lower bainite

reactions. In upper bainite the enriched austenite decomposed during subsequent tempering to ferrite and carbide; carbide precipitation was shown to occur at the austenite/ferrite interface and grow into the austenite. This behaviour is consistent with the crystallography of austenite, ferrite and carbide phases found, and conforms to a generally agreed sequence for the upper bainitic carbide precipitation reaction. It was not possible to determine whether the upper bainitic ferrite was supersaturated with carbon at any stage of its formation. This was possible to deduce, however, in the case of lower bainitic ferrite. Firstly, because of the mechanical twinning which implies a higher yield stress conferred by carbon supersaturation, and secondly, because of structural observations made of the mode of intralath carbide precipitation. This carbide was not observed at very short transformation times, but then precipitated on more than one variant of the habit plane, and with a uniquely determined habit plane consistent with minimum energy precipitation from supersaturated solid solution.

The absence of epsilon carbide and the thermal stability of lower bainitic cementite during retrogression experiments showed that the lower bainite reaction cannot in general be considered as a product of a metastable eutectoid reaction.

Table I.1

Austenitising Treatment	Grain Size/μm	P_{022_α}	Retained Austenite(%)
955°C @ 15 mins	35	0.629	22
955°C @ 15 mins	35	0.798	22
955°C @ 66 mins	45	0.631	20
955°C @ 300 mins	62	0.366	15
955°C @ 715 mins	70	0.986	24
1100°C @ 5 mins	62	0.196	12
1280°C @ 15 mins	1000	0.563	16

Notes

1) All the specimens were isothermally transformed at 350°C for 115 mins after austenitising.
2) It should be noted that the above texture analysis and the regression determinations presented in the text should only be taken to apply to the specific set of specimens used here. Because the texture parameter (P_{022_α}) takes no account of three dimensional texture variation, the results are unlikely to be general. Hence the regression analysis based on the above data can only serve to illustrate the trends involved. It is likely that specimens with other hot working histories (towards the achievement of the final specimen shape) will exhibit different values for the above parameters with respect to the surface used in the X-ray analysis.

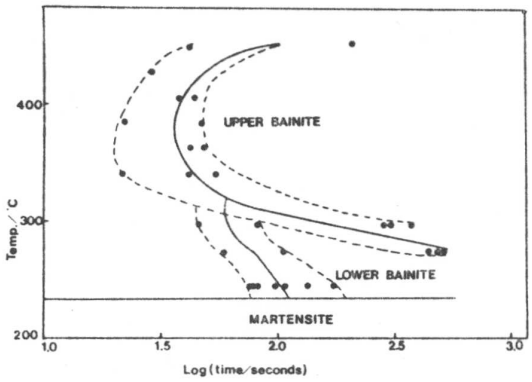

Figure I.1
Dilatometrically determined 5% transformation TTT curve.

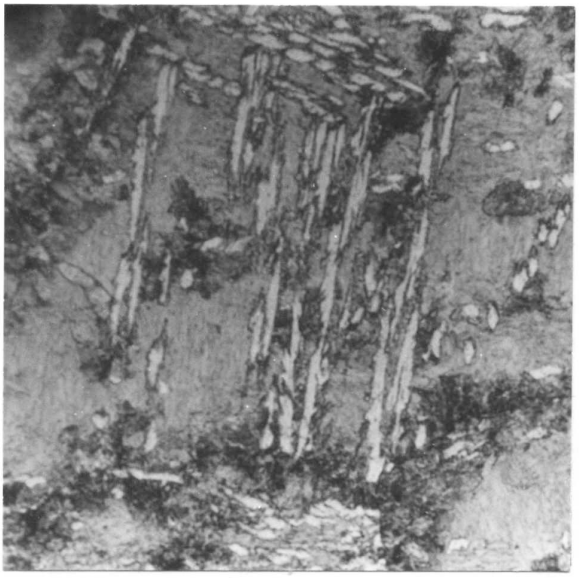

Figure I.2
Optical Micrograph showing the termination of the upper bainite reaction and the onset of pearlite formation after isothermal transformation at 452°C for 32 hours.

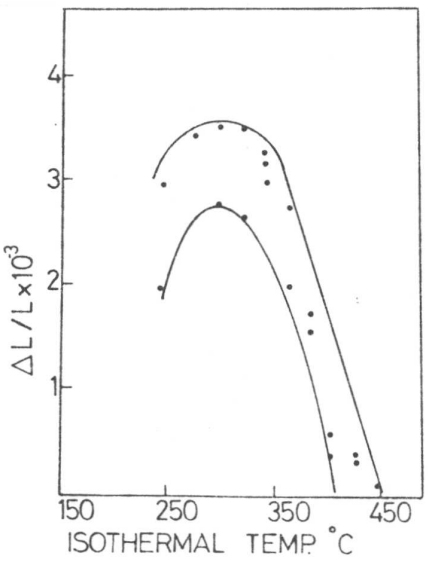

Figure I.3
Curve of dL versus isothermal transformation temperature showing temperature dependency of the 'incomplete reaction' phenomenon.

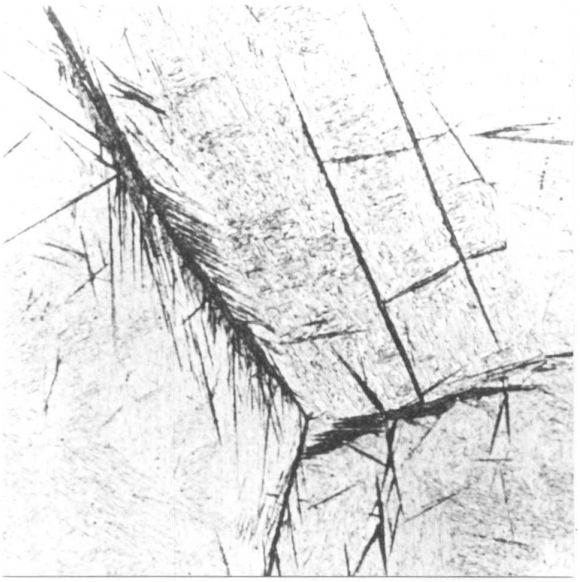

(a)

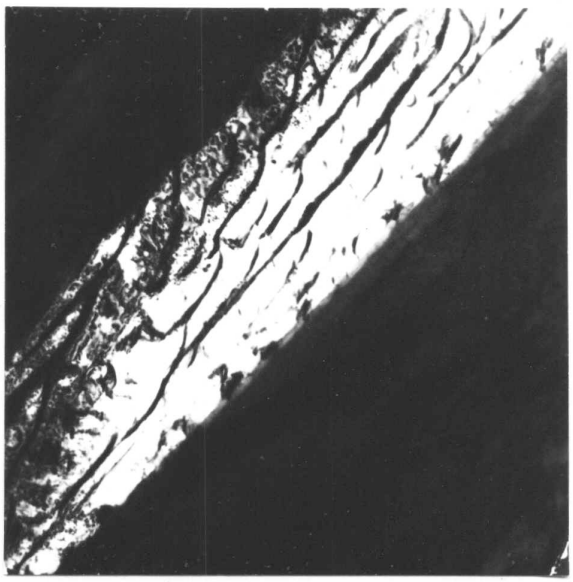

(b)

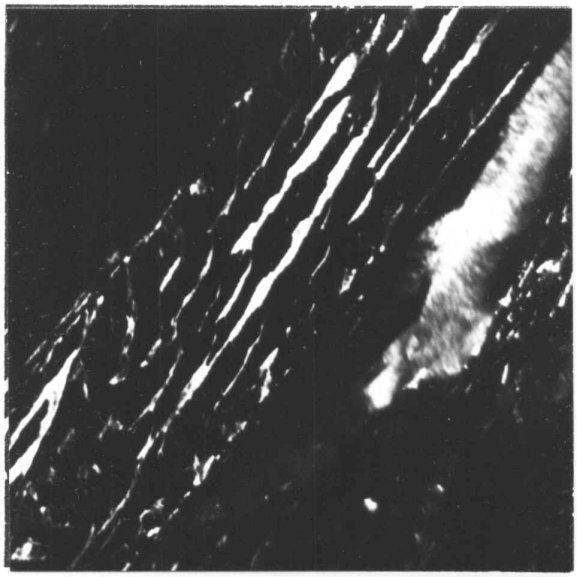

(c)

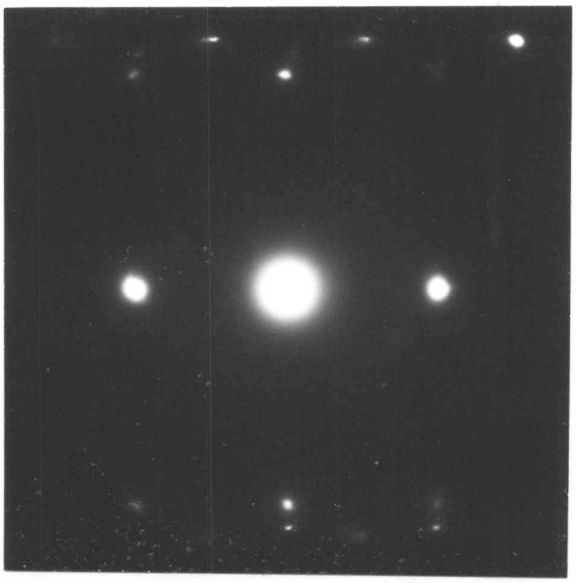

(d)

Figure I.4

Upper Bainite formed after isothermal transformation at 286°C for 30 minutes.

(a) Optical Micrograph.

(b) Transmission bright field image of a single 'plate'.

(c) Corresponding dark field image of retained austenite.

(d) Corresponding diffraction pattern.

(e) Interpretation of (d).

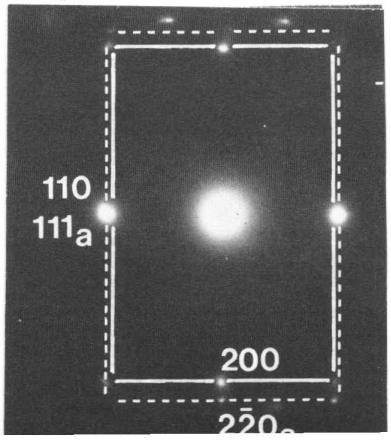

(e)

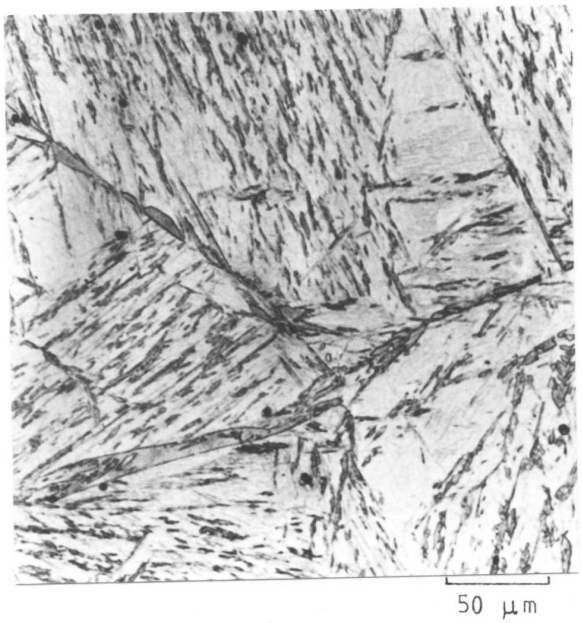

Figure I.5
Lower bainite formed after isothermal transformation at 246°C for 30 min.

Figure I.6
Upper bainite formed after isothermal transformation at 350°C for 205 min. The retained austenite is the grey phase.

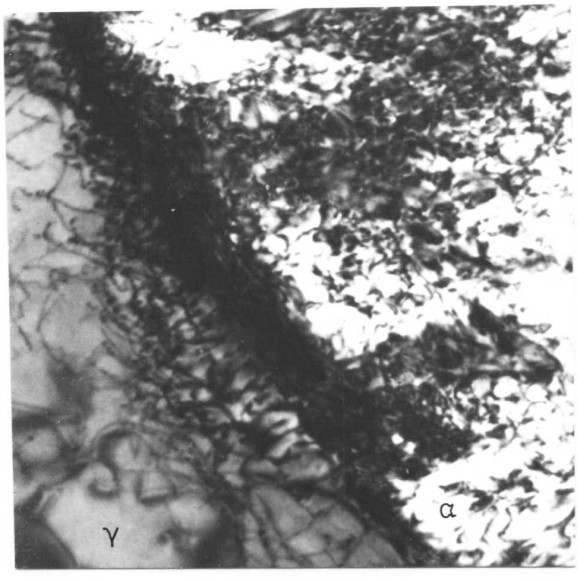

(a)

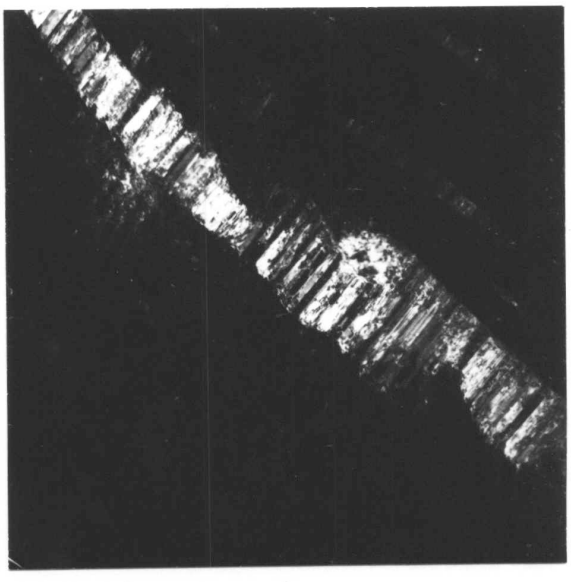

(b)

Figure I.7
Microstructural features of upper bainite formed after isothermal transformation at 350°C for 205 min.

(a) Dislocation clusters associated with the bainitic ferrite-retained austenite interface.

(b) Dark field image of upper bainitic retained austenite showing extensive faulting.

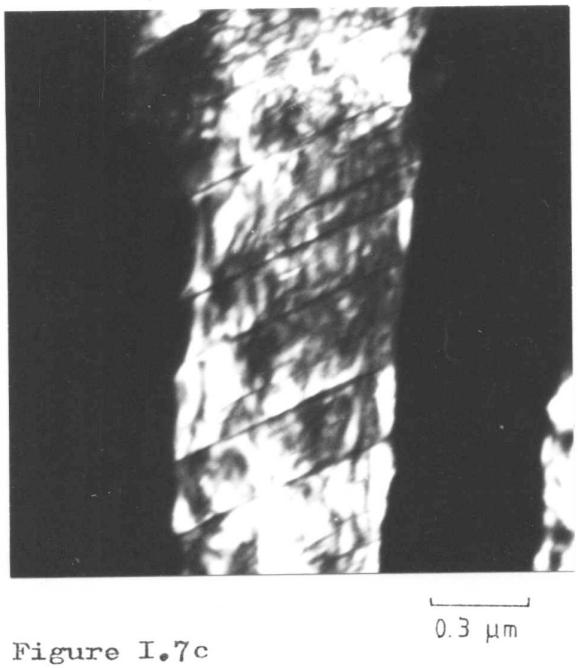

Figure I.7c
Dark field image of upper bainitic retained austenite showing accommodation slip steps. (Isothermally transformed at 350°C for 205 min.)

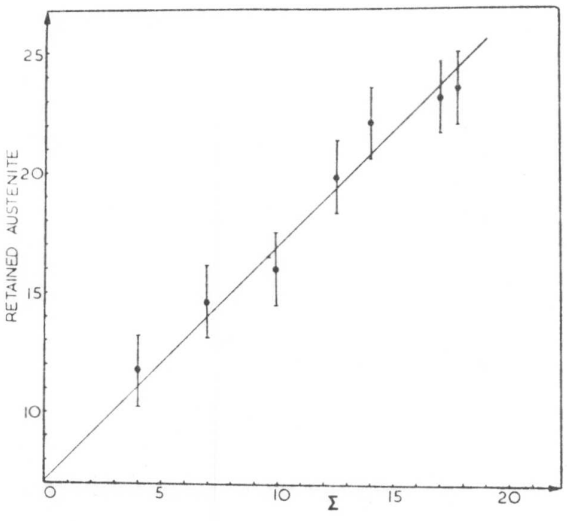

Figure I.8
The variation of upper bainitic retained austenite with the parameter Σ , where
$\Sigma = 17.5P_{022_\alpha} + (124000/d^3)$

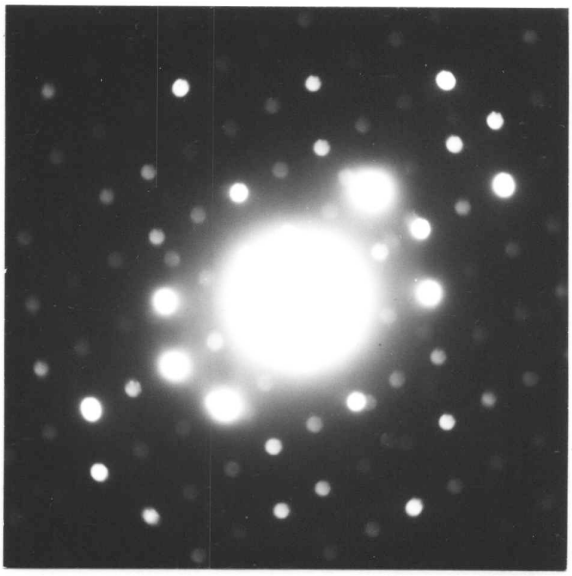

(a) (b)

Figure I.9
Precipitation events resulting from the tempering of upper bainite formed after isothermal transformation at 350°C for 205 min.
(a) Tempered at 500°C for 30 min.
(b) Convergent beam diffraction pattern from monoclinic carbide of the type illustrated in (9a).

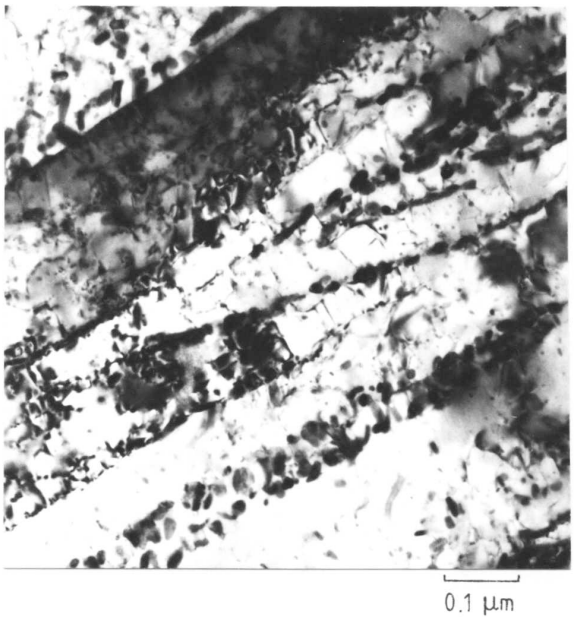

Figure I.9c
Tempered at 500°C for 60 min.

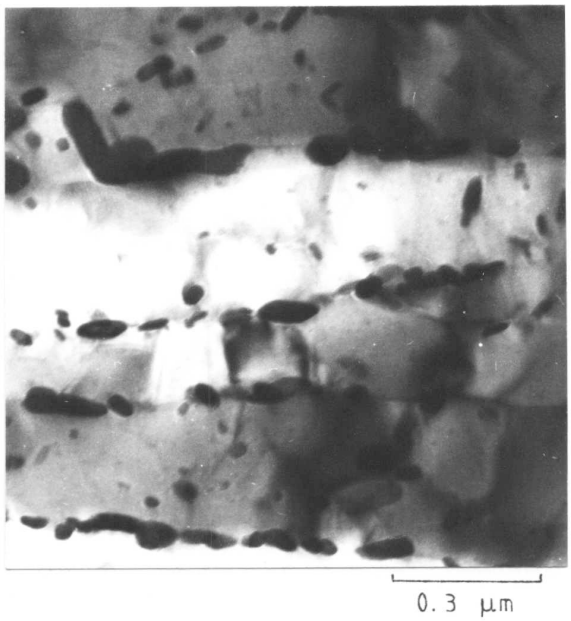

Figure I.9d
Tempered at 500°C for 120 min.

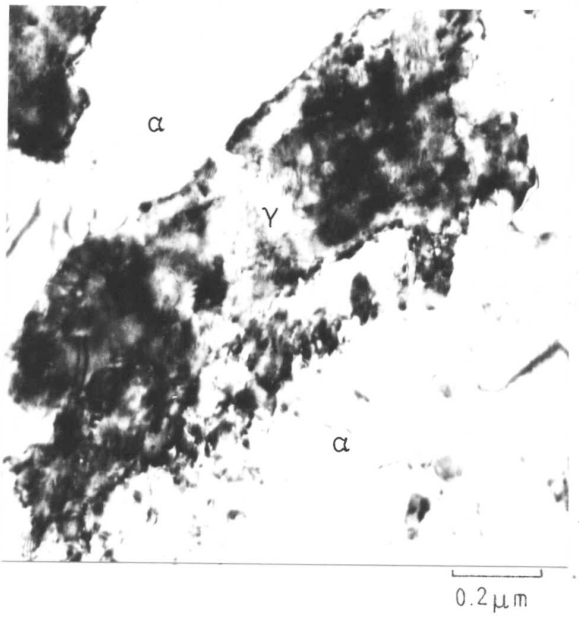

Figure I.9e
Hot stage electron micrograph showing decomposition of retained austenite at 500°C.

Figure I.10a
Typical lower bainitic microstructure after isothermal transformation at 300°C for 30 minutes.

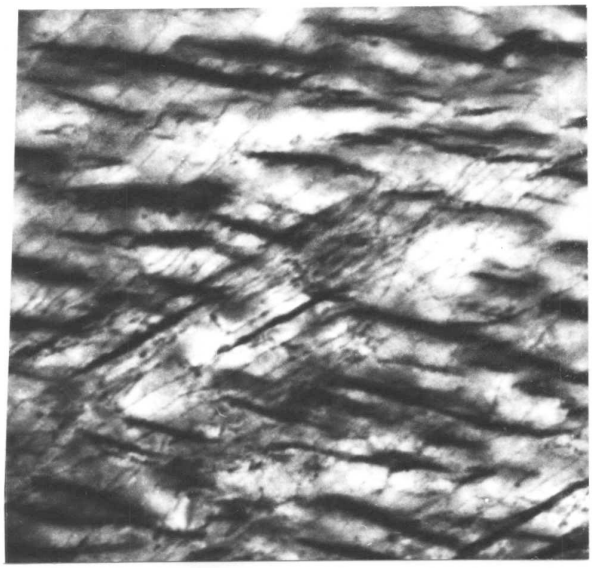

Figure I.10b
Dislocation arrays in lower bainitic ferrite formed after isothermal transformation at 247°C for 30 minutes.

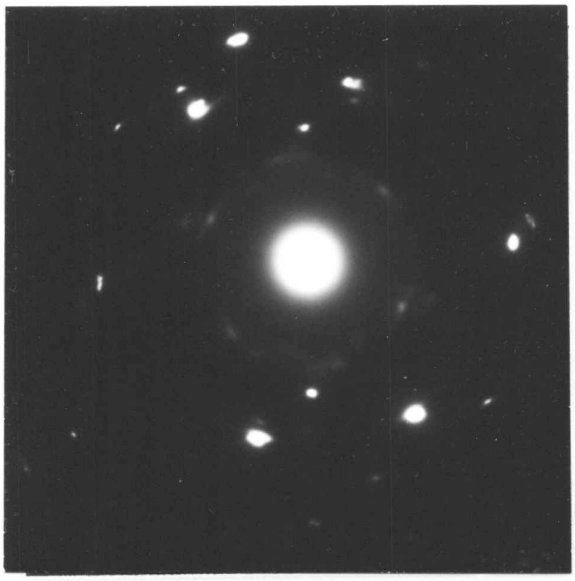

(i)

(ii)

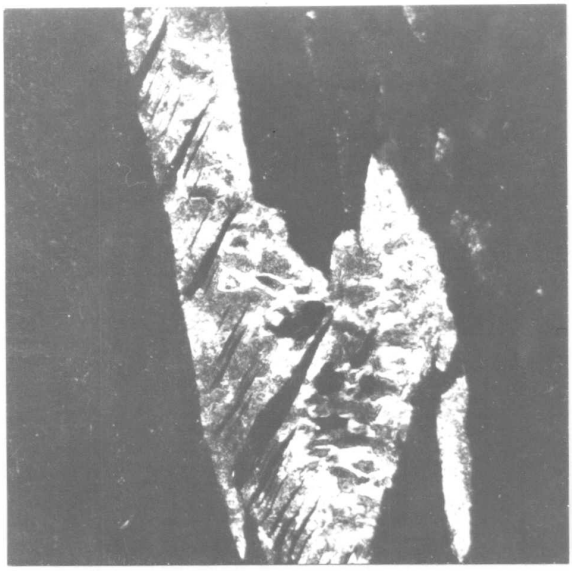

(iii)

(iv)

Figure I.10c

Mechanical twinning in lower bainite formed after isothermal transformation at 300°C for 30 minutes.

(i) Diffraction pattern.

(ii) Bright field image.

(iii) Matrix dark field image.

(iv) Twin dark field image.

(v) Interpretation of (i).

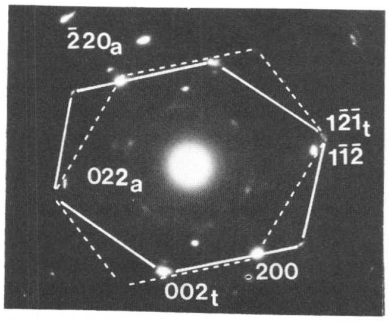

(v)

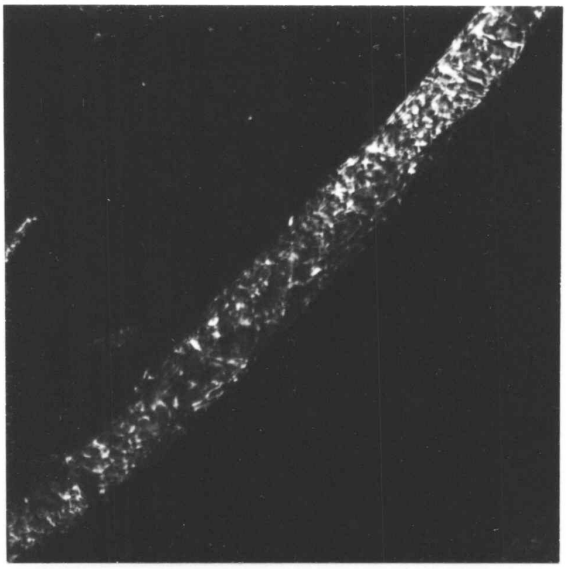

Figure I.10d
Structure of lower bainitic retained austenite after isothermal transformation at 300°C for 30 minutes.

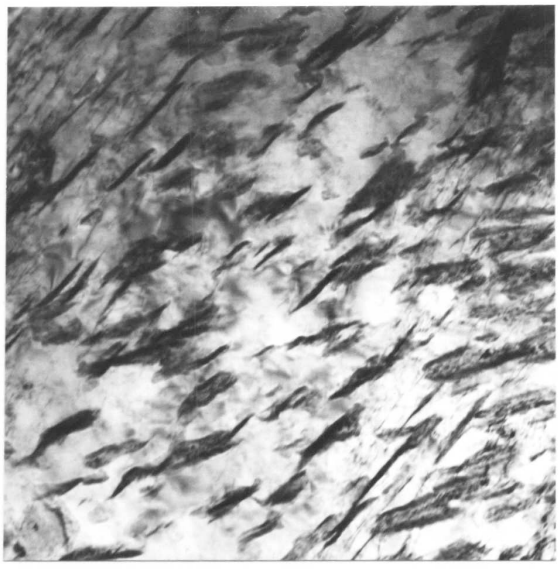

Figure I.10e
Morphology of lower bainitic cementite.

Figure I.11
Typical microstructure of lath martensite resulting from a direct quench following austenitisation.

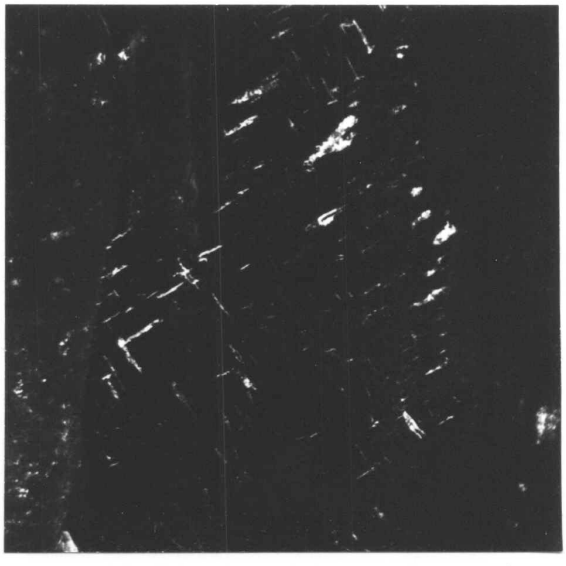

Figure I.12a
Dark field illumination of several cementite variants in a single ferrite crystal.

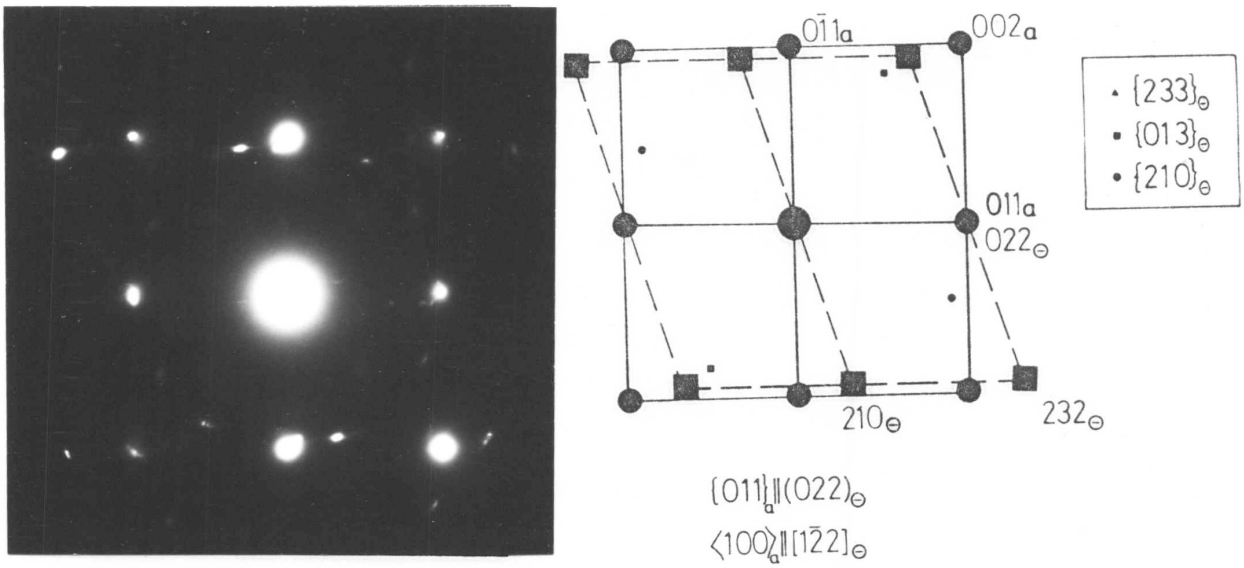

Figure I.12b
The orientation relationship between cementite and lower bainitic ferrite. It should be noted that $(011)_\theta$ is essentially a missing reflection.

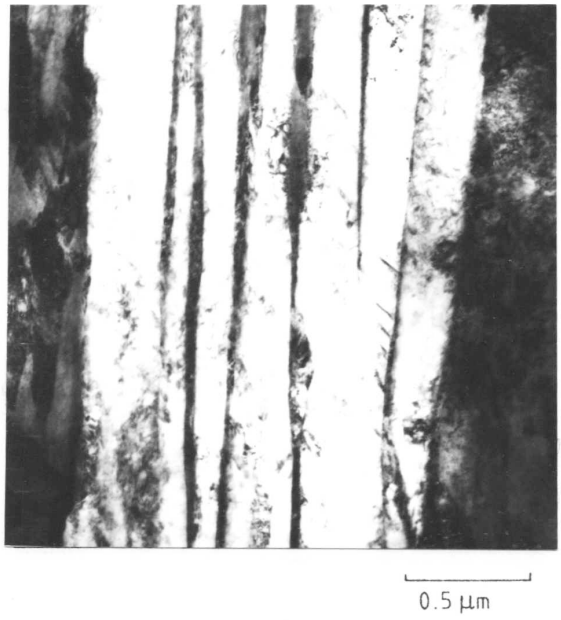

Figure I.12c
Incipient precipitation in lower bainite formed after isothermal transformation at 300°C for 4 minutes.

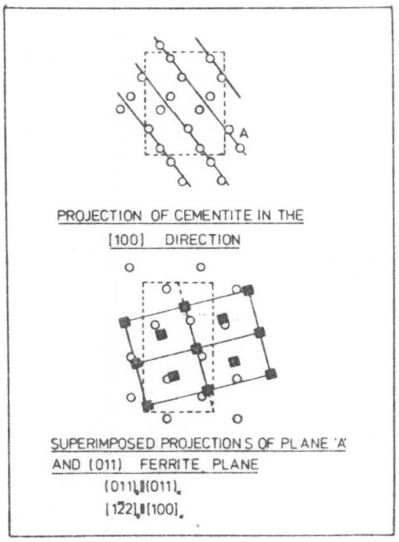

Figure I.12d
Superposition of iron atoms at the cementite-ferrite interface.

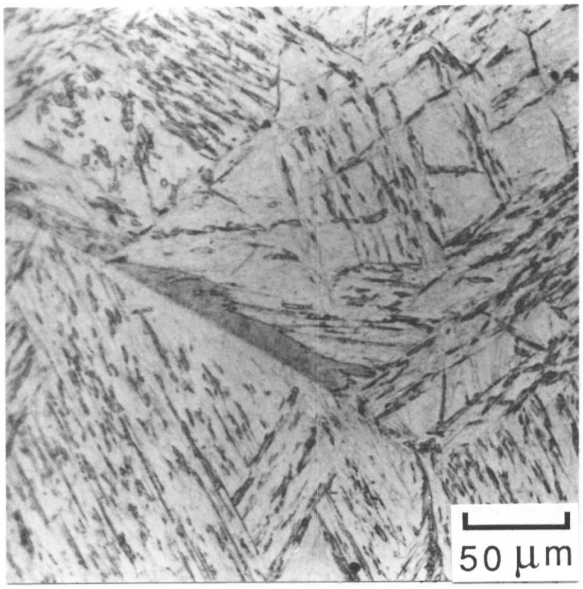

Figure I.13a
Grain boundary and intragranular lower bainite in a martensitic matrix after isothermal transformation at 246°C for 30 minutes.

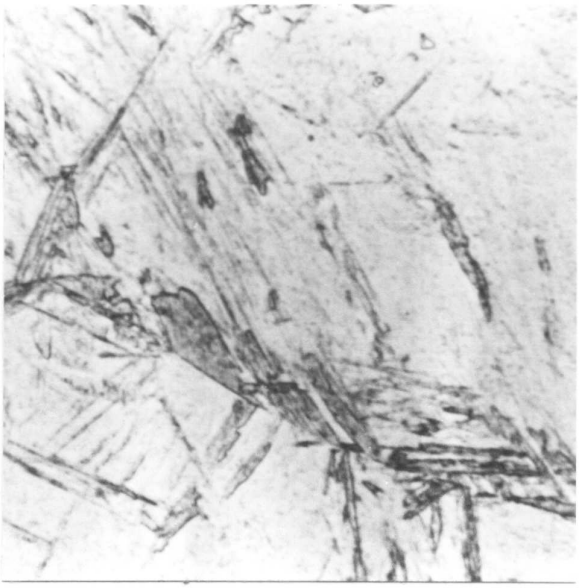

Figure I.13b
Parallelism of habit plane traces of grain boundary and intragranular lower bainite.

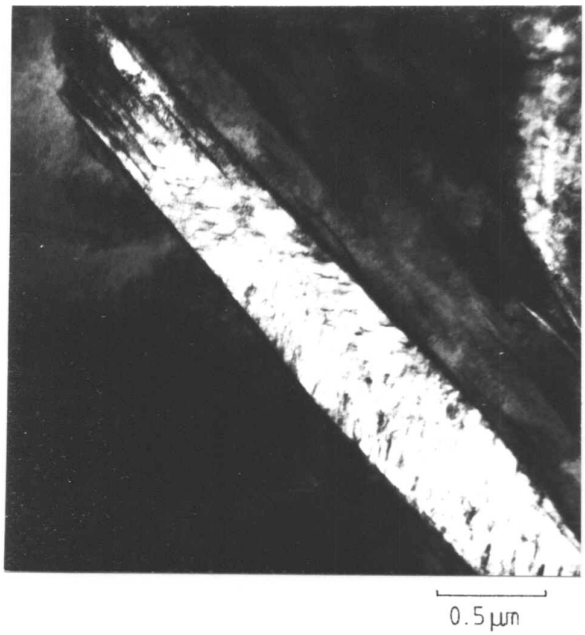

Figure I.13c
Structure of an intragranular plate tip; isothermally transformed at 257°C for 10 min.

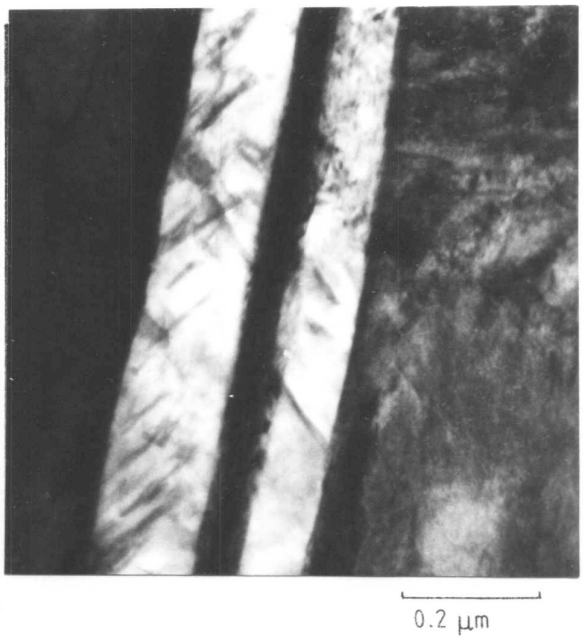

Figure I.13d
Individual spikes of lower bainite after isothermal transformation at 257°C for 5 min.

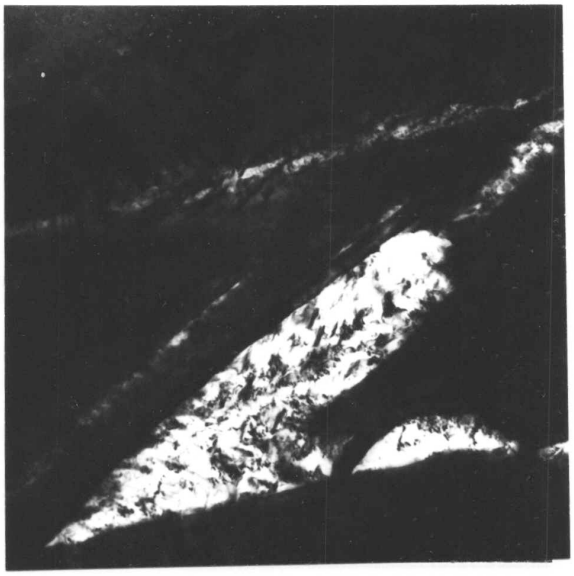

Figure I.13e
Spikes associated with grain boundary lower bainite formed during isothermal transformation at 257°C for 10 min.

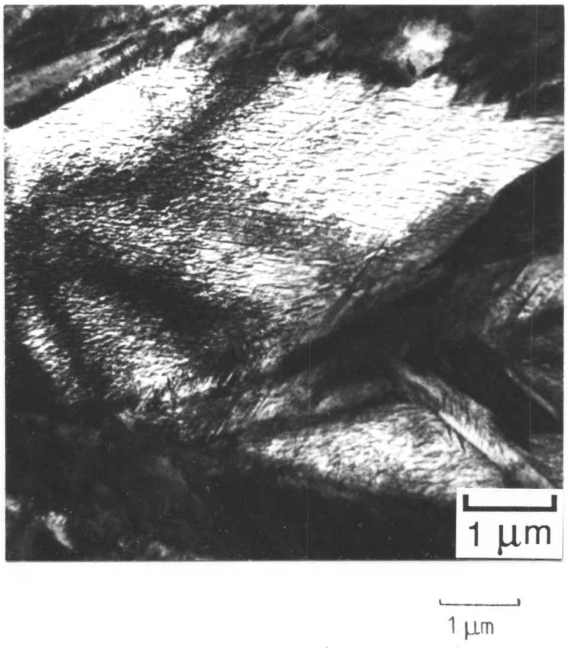

Figure I.13f
Grain boundary lower bainite formed during isothermal transformation at 247°C for 30 min.

KEY REFERENCES

1. R.F. Hehemann, K.R. Kinsman, H.I. Aaronson: Met. Trans., 1970, vol.3, pp.1077-1093.
2. H.I. Aaronson: 'The Mechanism of Phase Transformations in Crystalline Solids, Institute of Metals Monograph 33, 1968, p.270.
3. 1st Progress Report of Sub-Committee XI, ASTM Committee E-4; Proc. ASTM, 1950, vol.50, p.444.
4. 2nd Progress Report of Sub-Committee XI, ASTM Committee E-4; ibid., 1952, vol.52, p.543.
5. 4th Progress Report of Sub-Committee XI, ASTM Committee E-4; ibid., 1954, vol.54, p.568.
6. L. Habraken: Proc. 4th Int. Conf. on Electron Microscopy, 1958, p.621, Berlin.
7. R.M. Fisher: ibid., p.579.
8. F. B. Pickering: ibid., p.626.
9. K. Shimizu, Z. Nishiyama: Mem. Inst. Sci. Ind. Res. Osaka Univ., 1963, vol.20, p.43.
10. J.M. Oblak, R.F. Hehemann: 'Transformations and Hardenability in Steels' p.15, Climax Molybdenum Company, Ann Arbor, 1967.
11. B.A. Leontyev, G.V. Kovalevskaya: Phys. Met. Metallogr., 1974, vol.38, p.139.
12. N.A. Snurenskaya, L.I. Kogan, R.I. Etin: Phys. Met. Metallogr., vol.41, pp.1019 - 1028.
13. Der-Hung Huang, G. Thomas: Met. Trans., 1977, vol.8, p.1661.
14. N.F. Kennon: J. Aust. Inst. Metals, 1974, vol.19, pp.3 -18.
15. K.R. Kinsman, H.I. Aaronson: Transformations and Hardenability in Steels, p.39, Climax Molybdenum Company, Ann Arbor, 1967.
16. R.F. Hehemann: 'Phase Transformations', p.397, ASM, Metals Park, Ohio, 1970.
17. R. Le Houiller, G. Begin, A. Dube: Met. Trans., 1971, vol.2 p.2645.
18. N.F. Kennon: Met. Trans., 1978, vol.9, pp.57 - 66.
19. G.R. Purdy: Acta Met., 1978, vol. 26, pp.477 - 486.
20. G.R. Purdy: Acta Met., 1978, vol. 26, pp.487 - 498.
21. B. Uhrenius: Scand. J. Met., 1977, vol.6, pp.83 - 89.
22. G.R. Speich: 'Decomposition of Austenite by Diffusional Processes', p.353, Interscience Publishers, New York, 1962.
23. W.S. Owen: Trans. ASM, 1954, vol.46, pp.812 - 829.
24. J. Gordine, I. Codd: J.I.S.I., 1969, vol. 207.1, p. 461.
25. R.M. Hobbs, G.W. Lorimer, N. Ridley: J.I.S.I., 1972, vol.210.2, p.757.

26. M.J. Dickson: J. App. Cryst., 1969, vol.2, p.176, also, Private Communication, Dr. L. Remy, Ecole Nationale Superireure Des Mines de Paris, 91003 Evry Cedex, France. 1977.
27. B.D. Cullity: 'Elements of X-ray Diffraction', 1st Edition, p.334, Addison-Wesley Publishing Co., 1956.
28. G.B. Olson, M. Cohen: Met. Trans., 1976, vol.7, p.1797.
29. Y. Ohmori, R.W.K. Honeycombe: Supp. Trans. ISIJ, 1971, vol.11, p.1160.
30. K.W. Andrews: Acta Met., vol.11, 1963, p.939.
31. B. Jacobson, A. Westgren: Zietschrift fur Physikalische Chemie, Badenstein Anniversary Volume, 1931, p.177.
32. N.C. Law: Ph.D. Thesis, University of Cambridge, England, 1977.
33. H.I. Aaronson, M.R. Plichta, G.W. Franti, K.C. Russell: Met. Trans., 1978, vol.9, p.368.